DALTON
FULL PAPER

Oxidation of Tiron by (pyrophosphato)manganese(III). Kinetics and mechanism †

Imre Bozor and László I. Simándi *

Chemical Research Center, Institute of Chemistry, Hungarian Academy of Sciences, H-1525 Budapest, P.O. Box 17, Hungary. E-mail: simandi@chemres.hu

Received 14th May 2002, Accepted 14th June 2002
First published as an Advance Article on the web 22nd July 2002

The kinetics of oxidation of 4,5-dihydroxy-1,3-benzenedisulfonic acid (Tiron) by tris(pyrophosphato)manganese(III) in aqueous solution has been studied by the stopped-flow technique in the pH interval 1–6. Rapid-scan UV-Vis spectrophotometry in the 2–70 ms range revealed two parallel reactions, namely oxidation to the *o*-quinone and disproportionation to manganese(II) and soluble manganese(IV). The redox reaction exhibits first-order kinetics in both Mn^{III} and Tiron in the whole pH range investigated. The second-order rate constant shows a marked pH dependence with a maximum at pH = 2.4. The proposed reaction mechanism involves formation of two sets of Tiron–pyrophosphato–manganese(III) mixed-ligand intermediates, bonded *via* a catecholato or *via* a sulfonato group, respectively. They decompose to the quinone or the Mn(IV)/Mn(II) product in a rate-determining electron transfer or disproportionation. Remarkably, disproportionation is also first-order in both reactants, which implies a novel type of catalysis by Tiron, due to the greater substitutional lability of sulfonato *vs.* catecholato bonded Tiron.

Introduction

The oxidation of catechol derivatives attracts continuing interest owing to extensive studies related to the bioinorganic chemistry of catecholase and catechol dioxygenase type metalloenzymes and model systems.[1–3] The predominant metals involved in these systems are copper and iron, but recently a manganese catecholase has also been reported.[4] The redox interaction between manganese(III) and the 1,2-dihydroxybenzene moiety in aqueous solution is of interest in this context, with special reference to the mechanism of electron transfer. Tiron (4,5-dihydroxy-1,3-benzenedisulfonic acid), a water soluble substituted catechol is a suitable substrate for kinetic studies of its oxidation by the tris(dihydrogen pyrophosphato)manganese(III) complex. Tiron was reported to be a substrate for mushroom tyrosinase[5] due to its catecholase activity.

The coordination chemistry of Mn(III) in aqueous solution has been reviewed by Davies.[6] Aquamanganese(III) is a powerful oxidant in strong acid (E° = 1.56 V in 3 M $HClO_4$).[7] The redox potential is considerably reduced upon complexation with pyrophosphate (E° = 1.15 V),[8] or edta (E° = 0.824 V).[9]

Oxidations by manganese(III) and its complexes have been reviewed.[10] The oxidation of substituted benzene-1,2-diols[11] by aquamanganese(III) and its complexes with edta and cydta (cydta = cyclohexylenediaminetetraacetic acid)[12] has been studied in aqueous solution.

Manganese(III) has been demonstrated to be an intermediate in the oxidation of olefins and acetylenes by permanganate ion carried out in acidic aqueous solutions.[13]

In kinetic studies aimed at elucidating the mechanisms of permanganate ion oxidation of olefins and acetylenes, it was convenient to use pyrophosphate as a scavenger of Mn(III) to prevent its disproportionation to Mn(II) and MnO_2. The rapid formation of (pyrophosphato)manganese(III) and its low reactivity toward the starting olefins and the organic intermediates, facilitated efficient trapping and identification of the steps involved in the Mn(VII) ⟶ Mn(III) transformation.[13] In some cases, however, (pyrophosphato)manganese(III) exhibited remarkable reactivity, especially if the substrate and/or intermediates contained adjacent oxygen functionalities, like *e.g.* in benzene-1,2-diol derivatives. Except for a few scattered cases,[14] there is a general lack of mechanistic information for oxidations by (pyrophosphato)manganese(III).

We have therefore undertaken a detailed kinetic study of the oxidation of Tiron by (pyrophosphato)manganese(III). The results are reported in this paper.

Experimental

Manganese(III) acetate dihydrate, $Mn(OAc)_3{\cdot}2H_2O$ (Aldrich), was dissolved in water in the presence of a 10-fold molar excess of $Na_4P_2O_7{\cdot}10H_2O$ (Aldrich). Stock solutions were made up after filtering and were analysed iodometrically. The oxidant thus prepared corresponds to $[Mn(H_2P_2O_7)_3]^{3-}$ in acidic solution.[8,15] Tiron (4,5-dihydroxy-1,3-benzenedisulfonic acid, disodium salt monohydrate) was an Aldrich product.

UV-VIS spectra were recorded on a Hewlett-Packard 8453 diode array spectrophotometer. The pH was measured with a Radelkis OP 211/2 instrument. The kinetics were followed in an Applied Photophysics DX.17MV Bio-Sequential stopped flow spectrofluorimeter, which was also used for repetitive rapid scan spectrophotometry in the 1–1000 ms range. The UV-Vis spectra of Tiron oxidation products were monitored by the stopped-flow technique at various pHs. The method of generating time-dependent spectra by the stopped-flow device used involves the utilisation of absorbance *vs.* time traces recorded at various wavelengths. Spectra corresponding to given times after mixing are computed from these traces. These spectra are overlayed to produce the time evolution of successive spectra during the reaction.

The pH of both reactant solutions to be mixed in the stopped flow device was adjusted to the same value using a suitable buffer (Britton–Robinson) and also measured after the reaction in the effluent. The buffer concentration was adjusted so that the three pH values measured for each run agreed within

† Electronic supplementary information (ESI) available: kinetic data. See http://www.rsc.org/suppdata/dt/b2/b204678d/

 DOI: 10.1039/b204678d

0.01 pH units. Perchloric acid and NaOH were used to adjust the pH. The ionic strength (I) was kept at 0.50 M with $NaClO_4$.

Results and discussion

Stoichiometry

In acidic solution (pH < 2) Tiron is rapidly oxidised by $[Mn(H_2P_2O_7)_3]^{3-}$ to the corresponding *o*-quinone (TQ^{2-}). The stoichiometry [eqn. (1)] was determined by spectrophotometric titration based on the known spectra of the 4,5-quinone formed from Tiron (λ_{max} = 370 nm).[5]

The primary product TQ^{2-} is unstable, undergoing oligomerisation in a slower secondary non-redox reaction.[5] All of our kinetic results refer to the fast redox reaction.

Protonation equilibria of the reactants

Both oxidant and reductant may be involved in protonation/deprotonation equilibria, which are expected to affect the kinetic behaviour in the pH range used.

The predominant manganese(III) species in the presence of excess pyrophosphate over Mn(III) is the tris(dihydrogen pyrophosphato) complex,[8,15] $[Mn(H_2P_2O_7)_3]^{3-}$.

In order to obtain information about the protonation equilibria of (pyrophosphato)manganese(III) complexes, we have recorded the UV-VIS spectra in the pH interval from 2 to 6. The spectra obtained fall into two pH ranges differing in the magnitude of absorbance changes: (i) at pH 1.67–4.00 the spectral changes are significant (Fig. 1A), but (ii) above pH 4.30 only very slight spectral changes take place (Fig. 1B).

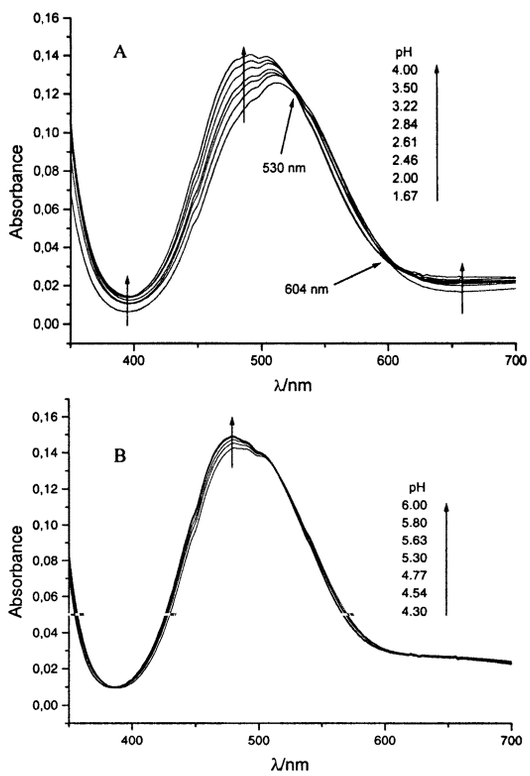

Fig. 1 Spectra of 1.4 mM $[Mn(H_2P_2O_7)_3]^{3-}$ and 14 mM $Na_4P_2O_7$ aqueous solutions as a function of pH. A: pH 1.67–4.00; B: pH 4.30–6.00.

The set of spectra in Fig. 1A exhibit two isosbestic points (530 and 604 nm), consistent with a single pH-dependent equilibrium. The major spectral changes occur around 500 nm.

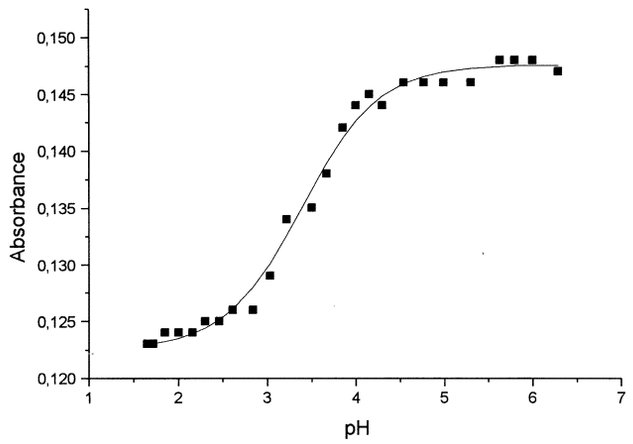

Fig. 2 Dependence of the absorbance at 480 nm on the pH. Solid line: curve calculated by a least-squares fit of eqn. (6) to the data. For the constants see Table 1

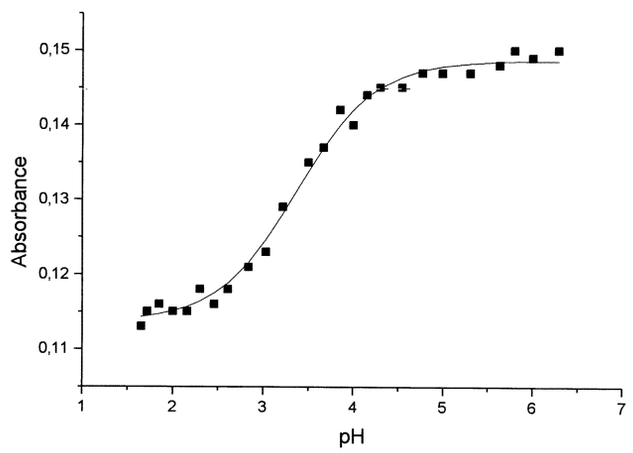

Fig. 3 Dependence of the absorbance at 490 nm on the pH. Solid line: curve calculated by a least-squares fit of eqn. (6) to the data. For the constants see Table 1.

Table 1 Protonation constant K_{23} and molar absorptivities ε_1 and ε_2 obtained from the least-squares fit of eqn. (6) to the experimental A *vs.* pH curves

λ/nm	ε_1/M^{-1} cm^{-1}	ε_2/M^{-1} cm^{-1}	K_{23}^{Mn}/M^{-1}
480	107 ± 2	81.3 ± 1.9	(2.52 ± 0.08) × 10^3
490	105 ± 2	87.1 ± 1.9	(2.65 ± 0.08) × 10^3
			Av. (2.58 ± 0.08) × 10^3

The pH dependences of the absorbance at λ = 490 and 480 nm are displayed in Figs. 2. and 3. At both wavelengths the absorbance changes according to a sigmoid curve, suggesting the involvement of a single protonation equilibrium (two absorbing species). The most likely process appears to be the deprotonation of $[Mn(H_2P_2O_7)_3]^{3-}$ at a non-coordinated –POH moiety as shown by eqns. (2) and (4).

The spectra of solutions with pH 4.30–6.00 (Fig. 1B) are very close to each other and to the pH 4 spectrum in Fig. 1A (depending on the wavelength, the maximum absorbance changes over the whole pH range are less than *ca.* 0.007–0.012). Nevertheless, isosbestic points in Fig. 1B are apparent at 386, 513 and 630 nm, indicating another equilibrium with two absorbing species. The nature of this equilibrium was not investigated further because of the lack of sufficiently accurate spectral data. It might be associated with deprotonation of another coordinated $H_2P_2O_7^-$ ligand similar to reaction (2).

$$\underset{(H_2T^{2-})}{(HO)_2C_6H_2(SO_3)_2^{2-}} + 2[Mn(H_2P_2O_7)_3]^{3-} \rightarrow \underset{(TQ^{2-})}{(O)_2C_6H_2(SO_3)_2^{2-}} + 2[Mn^{II}(H_2P_2O_7)_3]^{4-} + 2H^+ \quad (1)$$

$$Mn_1 \rightleftarrows Mn_2 + H^+ \quad (2)$$

$$K_{23}^{Mn} = [Mn_1]/[Mn_2][H^+] \quad (3)$$

where

$$Mn_2 = [Mn(HP_2O_7)(H_2P_2O_7)_2]^{4-} \text{ and } Mn_1 = [Mn(H_2P_2O_7)_3]^{3-} \quad (4)$$

with the $HP_2O_7^{3-}$ ligand corresponding to triply deprotonated pyrophosphoric acid, and

$$[Mn^{III}]_T = [Mn_1] + [Mn_2] \quad (5)$$

The continuous line drawn through the points corresponds to the least-squares fit of eqn. (6) to the experimental points.

$$A_\lambda = [Mn]_T \frac{\varepsilon_1 + \varepsilon_2 K_{23}^{Mn}[H^+]}{1 + K_{23}^{Mn}[H^+]} \quad (6)$$

The best-fit values of the three parameters of eqn. (6) at 480 and 490 nm are listed in Table 1. Equilibrium (2) will be considered when interpreting the pH dependence of the observed rate constant for the oxidation of Tiron.

Rapid scan spectrophotometry

The spectral changes (in the 330–670 nm interval) accompanying the reaction were monitored by the stopped-flow/repetitive scan technique in the 1–77 ms range at pH 1.2–6.0. Typical sets of overlaid spectra are shown in Fig. 4. From pH 1.49 to 3.57 the 370 nm band increases in each run, revealing the formation of the quinone product.[5] Two isosbestic points (at 340 and 445 nm) are apparent at pH 1.49 and 2.14, indicating that quinone formation step (1) is the only reaction occurring in this pH interval. From pH 2.86 the isosbestic points are gradually lost and two others (480 and 555 nm) begin to develop. At the high end of the pH range studied the 370 nm quinone band is completely absent. The spectral changes observed in this pH interval are consistent with *another reaction*, which should be the disproportionation of tris(pyrophosphato)manganese(III): the 505 nm band of $[Mn(H_2P_2O_7)_3]^{3-}$ gives way to the featureless spectrum of soluble Mn(IV), exhibiting monotonically increasing absorbance with decreasing wavelength. Remarkably, solutions of $[Mn(H_2P_2O_7)_3]^{3-}$ are stable for hours *in the absence of* H_2T^{2-}, exhibiting *no time-dependent spectral changes* at the pH values used in the runs of Fig. 4. This implies that Tiron is responsible for the second reaction, which can thus be regarded as Tiron-catalysed disproportionation of $[Mn(H_2P_2O_7)_3]^{3-}$. In the pH range of 4–5 it can be written as eqn. (7), which indicates only the relevant redox changes.

$$2[Mn(H_2P_2O_7)_3]^{3-} \xrightarrow{H_2T^{2-}} [Mn^{II}(H_2P_2O_7)_3]^{4-} + Mn(IV)_{sol} + 3 \text{ pyrophosphate} \quad (7)$$

Our attempts at detecting free radical species in the reaction mixture by ESR spectroscopy failed, indicating that the concentration and/or lifetime of the expected semiquinone anion radical is too low/short for detection by the technique used.

Kinetic measurements

The kinetics of the parallel reactions (1) and (7) was followed by stopped-flow spectrophotometry in the wavelength range of 325–625 nm. Pseudo first-order conditions were ensured by using a 10-fold or greater excess of H_2T^{2-} over $[Mn(H_2P_2O_7)_3]^{3-}$ in terms of eqn. (1).

Individual absorbance *vs.* time traces were recorded at 370 and 505 nm. These are characteristic wavelengths corresponding to TQ^{2-} and $[Mn(H_2P_2O_7)_3]^{3-}$, respectively. At 370 nm the absorbance rapidly increases with time and, after reaching a maximum at about 100–200 ms, it starts to slowly decrease due to oligomerisation of the quinone formed.[5] Our kinetic measurements refer to the fast redox reaction before the maximum. At 505 nm the absorbance monotonically decreases with time over about 100–200 ms.

In a few experiments, the spectral changes due to the slow reaction after the maximum were monitored for 2–3 hours. Isosbestic series of spectra indicated a single reaction, previously described[5] as the dimerisation of TQ^{2-}, which was not further investigated.

First-order kinetic behaviour was observed at both wavelengths throughout the pH range studied, as demonstrated by excellent single-exponential fits of the kinetic traces by the instrument software. The *A vs.* time curves at 370 nm were fitted up to the maximum with a single exponential function using the instrument software. It was possible to extend the fitting beyond the maximum by including a linear component into the fitting function, which accounted for the slow decrease of absorbance after the maximum.

Test runs were carried out to see if atmospheric O_2 has any effect on the rate. Kinetic runs with N_2-saturated (deaerated) solutions in the reservoir syringes of the stopped-flow device afforded the same rate constants as obtained in runs under air.

Variation of the overall pyrophosphate concentration from 7 to 25 mM at constant Mn(III) concentration (0.5 mM) at various pHs did not change the rate constant beyond the experimental error. The buffer concentration had no appreciable effect on the rate either. A 3-fold increase in the ionic strength increased the rate by *ca.* 10%, as expected for a reaction between ionic species of like charge.

The observed first-order rate constant k_{obs} is proportional to the concentration of H_2T^{2-} if the latter is present in a 10–24-fold excess, and a 10-fold excess of pyrophosphate over Mn(III) is maintained. The dependence of k_{obs} on the Tiron concentration is shown in Fig. 5 at selected pHs for absorbance at 370 nm. Similar behaviour was observed at 505 nm. The second-order rate constant k calculated from eqn. (8) for both

$$k_{obs} = k[H_2T^{2-}]_0 \quad (8)$$

the 370 and 505 nm traces shows distinct pH-dependence with maxima around pH 2.5 (Fig. 6).

The *k vs.* pH profiles are remarkably different in height (but similar in shape) for the two wavelengths, indicating that the stopped-flow traces monitor different sets of reactions (Fig. 4).

The observed kinetic behaviour and the pH dependence of the second-order rate constant can be interpreted in terms of the following proposals. The protonation equlibria (9) and (11) of the two SO_3H groups of Tiron involve a total of three species, H_4T, H_3T^- and H_2T^{2-}, with pK_1 and pK_2 values on the low-pH side of the maximum in Fig. 6 (pK_1 = 1.02; pK_2 = 1.70; pK_3 = 8.60; pK_4 = 14.5).[16] The decrease of k on the high-pH side is ascribed to hydrolysis/deprotonation equilibrium (2) of tris(pyrophosphato)manganese(III), which generates an additional, less reactive Mn^{III} species. (No more Tiron species are possible below pH 6 in view of its pK.) The three Tiron and two Mn^{III} species correspond to a total of six possible redox routes for the overall reaction studied.

$$[H_2T^{2-}] + H^+ \rightleftarrows [H_3T^-] \quad (9)$$

$$K_{23}^{T} = [H_3T^-]/[H_2T^{2-}][H^+] \quad (10)$$

An important assumption is that the redox reactions between Mn(III) and Tiron species should be much slower than the

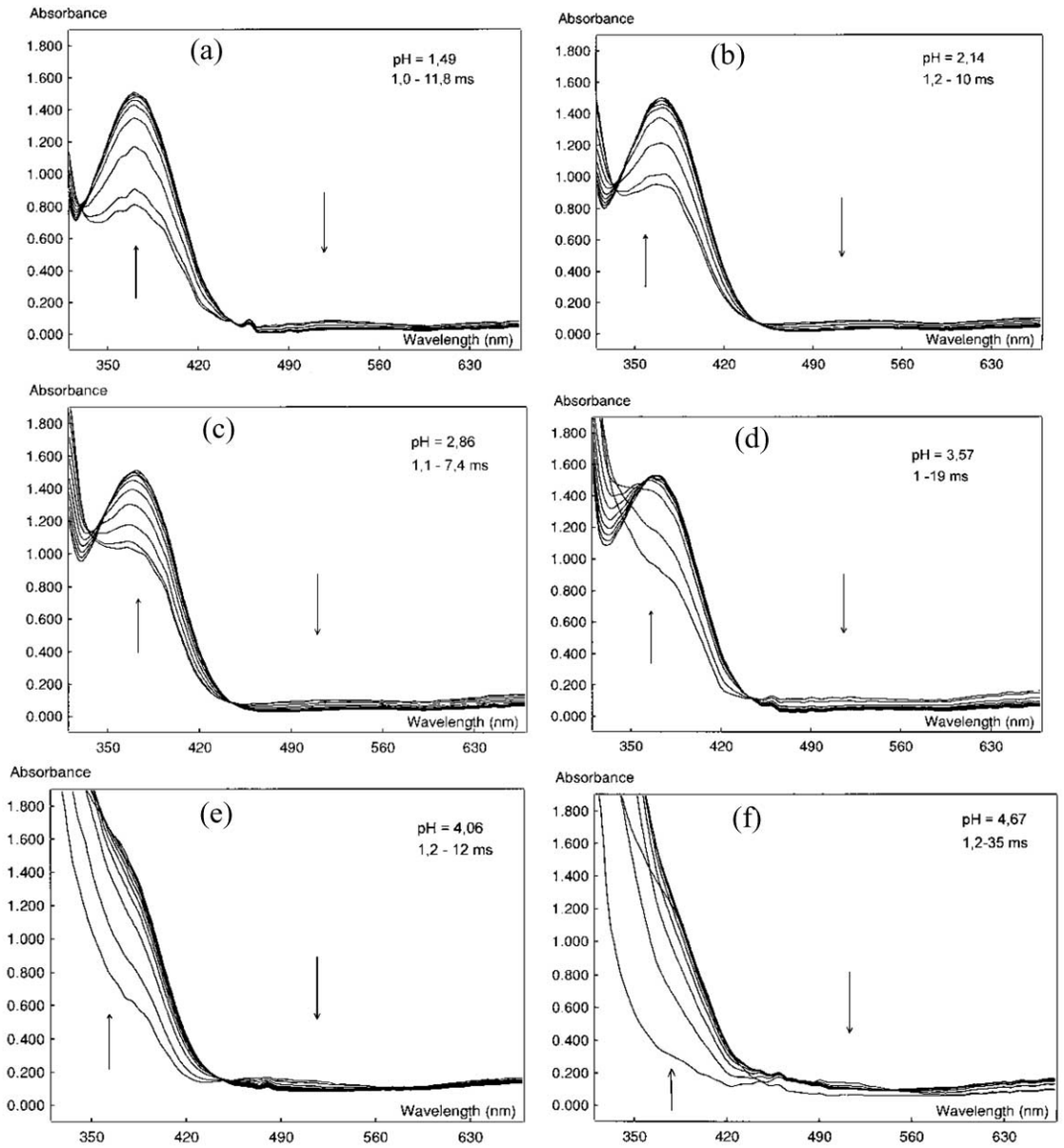

Fig. 4 Time evolution (1.12–35 ms) of the UV-Vis spectra corresponding to the oxidation of Tiron by (pyrophosphato)manganese(III), as monitored by rapid scan spectrophotometry using the stopped-flow device. $[Mn]_T = 1.3$ mM, $[T]_0 = 20$ mM; $I = 0.5$ M, [Buffer] = 0.08 M, pH (a) 1.49, (b) 2.14, (c) 2.86, (d) 3.57, (e) 4.06, (f) 4.67; $T = 25$ °C.

protonation/deprotonation steps, therefore, (2), (9) and (11) behave as pre-equilibria, which depend solely on the pH.

$$[H_3T^-] + H^+ \rightleftarrows [H_4T] \quad (11)$$

$$K_{34}^{T} = [H_4T]/[H_3T^-][H^+] \quad (12)$$

The kinetics of the two parallel reactions (1) and (7) are identical, being first-order in both Tiron and Mn(III), and pH dependencies due to coupled protonation/deprotonation equilibria. The *k vs.* pH profiles at 370 an 505 nm merge at both ends of the pH scale (*ca.* 1 and 6), where identical rate constants are observed at both wavelengths, indicating that only one of the two parallel reactions contributes: at pH < 1.5 only oxidation (1), whereas at pH > 4.5 only disproportionation (7) takes place. At intermediate pHs both reactions occur. The *k* values at 370 and 505 nm include pH-dependent contributions from (1) and (7).

The proposed reaction mechanism is shown in Scheme 1. As a consequence of protonation equilibria (2), (9) and (11), there are a total of two Mn^{III} and three Tiron species in solution. Each one of the intermediate complexes X_1–X_8 is formed in the appropriate pre-equilibrium from one Mn^{III} and one Tiron species. Complex formation presumably occurs *via* displacement of one coordinated pyrophosphato –P–O$^-$ group by an

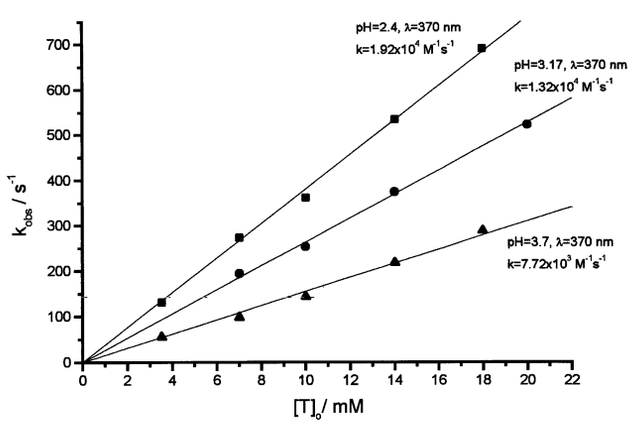

Fig. 5 Dependence of the first-order rate constant k_{obs} on the Tiron concentration at different pHs. 370 nm, $[Mn]_0 = 1.5$ mM; $[P_2O_7^{4-}] = 15$ mM, $T = 25$ °C, $I = 0.5$ M (also see Tables S1 and S2, ESI).

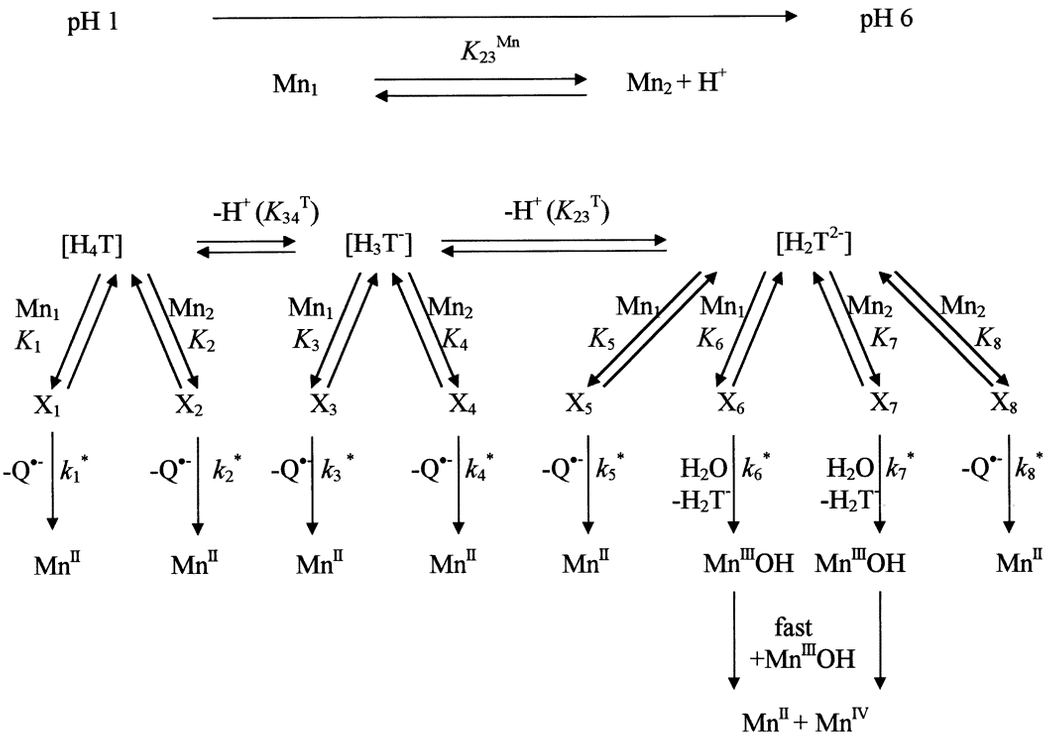

Scheme 1

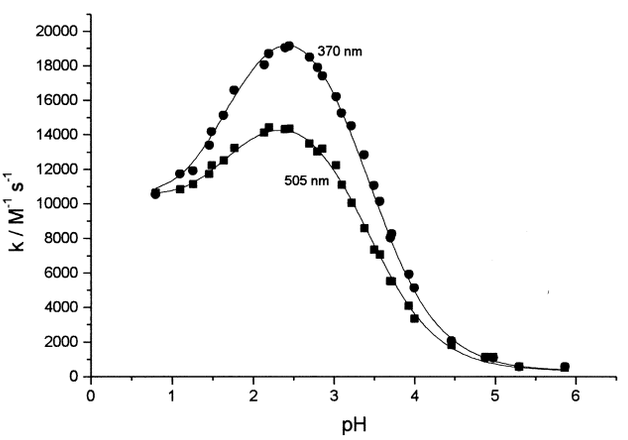

Fig. 6 Dependence of the second-order rate constant k on the pH at 370 and 505 nm. Conditions: $[Mn]_T$ = 1.5 mM, $[P_2O_7^{4-}]$ = 15 mM, T = 25 °C, I = 0.5 M (also see Table S3, ESI).

–OH or $–SO_2O^-$ group of Tiron. Accordingly, there are two kinds of X_i complexes, differing from each other in the type of Tiron to Mn^{III} bonding. As both the pyrophosphato and benzenediolato (H_2T^{2-}) ligands are bidentate, it is reasonable to picture the species X_1–X_8 as mixed-ligand complexes involving one ligand of both kinds coordinated in a unidentate fashion.

In intermediates X_1–X_5 and X_8 bonding is through an aromatic $–O^-$ group, generated *via* deprotonation of an –OH group by the $–PO^-$ group displaced, Scheme 2). In X_6 and X_7, bonding is through an $–SO_2O^-$ group displacing a $–PO^-$ group (Scheme 3). To our knowledge, this type of metal–ligand bonding has not been observed or proposed thus far. The rate-determining redox decomposition of intermediates X_1–X_5 and X_8 involves inner-sphere[7] electron transfer and proton loss from Tiron –OH groups (for simplicity, not shown in Scheme 1), affording a semiquinone anion radical $TQ^{\bullet-}$. Alternatively, rate-determining hydrolysis of X_6 and X_7 generates a hydroxobis(pyrophosphato)manganese(III) species ($Mn^{III}OH$), which then undergoes rapid disproportionation to the observed soluble (pyrophosphato)manganese(IV) complex.

The oxidation and hydrolysis pathways are first-order in both Mn^{III} and Tiron, *i.e.* all of the transformations observed are kinetically equivalent to each other. The pH dependence observed is due to the coupled protolytic equilibria involving the oxidant and substrate species.

The remarkable catalytic effect of Tiron on the hydrolysis/disproportionation of $[Mn(H_2P_2O_7)_3]^{3-}$ must be due to the good leaving group properties of the $–SO_2O^-$-bonded Tiron relative to the pyrophosphato ligand. This is supported by the lack of $[Mn(H_2P_2O_7)_3]^{3-}$ hydrolysis in the absence of Tiron at identical pHs.

The relationship between the rate and equilibrium constants in Scheme 1 is

$$k_i = K_i k_i^* \ (i = 1,2,\ldots 8) \qquad (13)$$

The fast steps occurring after the above rate-determining steps are as follows. For routes *via* X_1–X_5 and X_8 (redox reactions):

$$TQ^{\bullet-} + Mn_1 \xrightarrow{\text{fast}} TQ^{2-} + Mn^{II} \qquad (14)$$

$$TQ^{\bullet-} + Mn_2 \xrightarrow{\text{fast}} TQ^{2-} + Mn^{II} \qquad (15)$$

For routes *via* X_6 and X_7 (hydrolysis/disproportionation):

$$2\,Mn^{III}OH \xrightarrow{\text{fast}} Mn^{IV} + Mn^{II} + 2OH^- \qquad (16)$$

The difference between the k *vs.* pH profiles obtained from kinetic runs at 370 and 505 nm (Fig. 6) may be, to a first approximation, due to the strong contribution of quinone oxidation to the 370 nm trace, and its negligible contribution to the 505 nm trace. Consequently, the 370 nm kinetic trace predominantly reflects oxidation to the quinone (1) together with a contribution from disproportionation (7), whereas the kinetic curves at 505 nm are mainly due to disproportionation (7). However, the two processes significantly overlap, therefore separation is only possible by a numerical fitting procedure.

Kinetic equation

The kinetic results are consistent with the mechanism in Scheme 1. The solid lines in Figs. 6 and 7 have been calculated

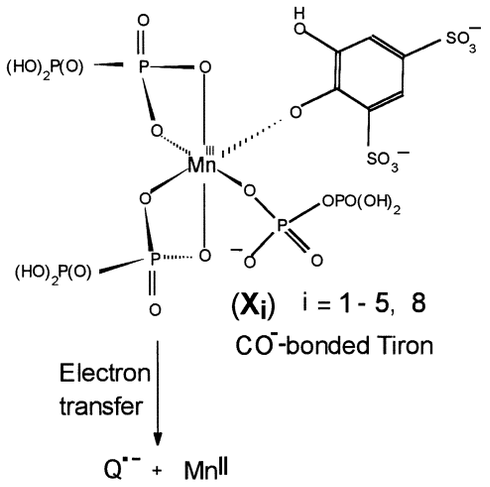

Scheme 2

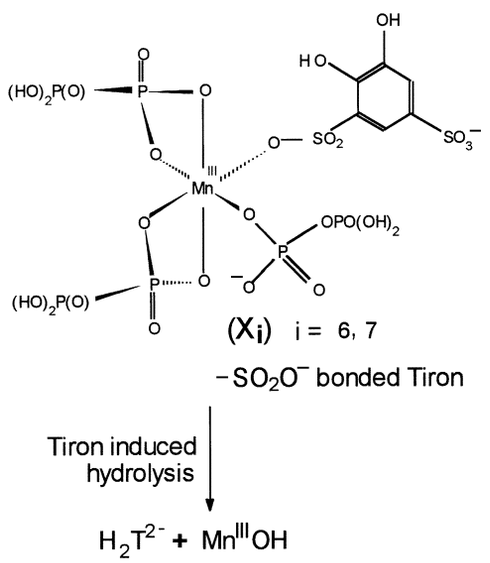

Scheme 3

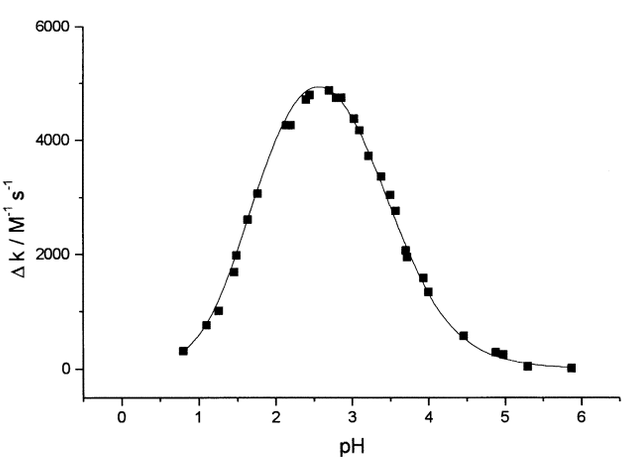

Fig. 7 Plot of $\Delta k = k_{370} - k_{505}$ against pH. The solid line was calculated from eqn. (29) using the constants in the last column of Table 2

from the kinetic equation derived thereof in the following way [*cf.* eqn. (31)].

According to Scheme 1, the overall rate of product formation is the sum of the individual (parallel) rate terms, eqn. (17).

$$\mathrm{d[P]/d}t = \{k_1[\mathrm{H_4T}] + k_3[\mathrm{H_3T^-}] + k_5[\mathrm{H_2T^{2-}}] + k_6[\mathrm{H_2T^{2-}}]\}[\mathrm{Mn_1}] + \{k_2[\mathrm{H_4T}] + k_4[\mathrm{H_3T^-}] + k_7[\mathrm{H_2T^{2-}}] + k_8[\mathrm{H_2T^{2-}}]\}[\mathrm{Mn_2}] \quad (17)$$

where

$$[\mathrm{P}] = [\mathrm{TQ^{2-}}] + [\mathrm{Mn^{IV}}] \quad (18)$$

is the sum of product concentrations.

The required species concentrations can be obtained from the mass balance eqns. (19) and (23) for Mn^{III} and Tiron, respectively, combined with expressions (3), (10) and (12) for the equilibrium constants.

$$[\mathrm{Mn^{III}}]_\mathrm{T} = [\mathrm{Mn_1}] + [\mathrm{Mn_2}] \quad (19)$$

$$[\mathrm{Mn_1}] = [\mathrm{Mn^{III}}]_\mathrm{T} K_{23}^{\mathrm{Mn}}[\mathrm{H^+}]/B \quad (20)$$

$$[\mathrm{Mn_2}] = [\mathrm{Mn^{III}}]_\mathrm{T}/B \quad (21)$$

where

$$B = 1 + K_{23}^{\mathrm{Mn}}[\mathrm{H^+}] \quad (22)$$

$$[\mathrm{T}]_\mathrm{T} = [\mathrm{H_2T^{2-}}] + [\mathrm{H_3T^-}] + [\mathrm{H_4T}] \quad (23)$$

$$[\mathrm{H_2T^{2-}}] = [\mathrm{T}]_\mathrm{T}/A \quad (24)$$

$$[\mathrm{H_3T^-}] = [\mathrm{T}]_\mathrm{T} K_{23}^{\mathrm{T}}[\mathrm{H^+}]/A \quad (25)$$

$$[\mathrm{H_4T}] = [\mathrm{T}]_\mathrm{T} K_{23}^{\mathrm{T}} K_{34}^{\mathrm{T}}[\mathrm{H^+}]^2/A \quad (26)$$

$$A = 1 + K_{23}^{\mathrm{T}}[\mathrm{H^+}] + K_{23}^{\mathrm{T}} K_{34}^{\mathrm{T}}[\mathrm{H^+}]^2 \quad (27)$$

Upon inserting the expressions for the concentrations of the reacting species into (17) and rearrangement, one obtains the full kinetic equation (28).

$$\mathrm{d[P]/d}t = \{(k_1 K_{23}^{\mathrm{Mn}}[\mathrm{H^+}] + k_2) K_{23}^{\mathrm{T}} K_{34}^{\mathrm{T}}[\mathrm{H^+}]^2 + (k_3 K_{23}^{\mathrm{Mn}}[\mathrm{H^+}] + k_4) K_{23}^{\mathrm{T}}[\mathrm{H^+}] + (k_5 + k_6) K_{23}^{\mathrm{Mn}}[\mathrm{H^+}] + k_7 + k_8\}[\mathrm{Mn^{III}}]_\mathrm{T}[\mathrm{T}]_\mathrm{T}/AB \quad (28)$$

From eqn. (28), the observed first- (k_{obs}) and second- (k) order rate constants can be written as in eqn. (29).

$$k = k_{\mathrm{obs}}/[\mathrm{T}]_\mathrm{T} = \{(k_1 K_{23}^{\mathrm{Mn}}[\mathrm{H^+}] + k_2) K_{23}^{\mathrm{T}} K_{34}^{\mathrm{T}}[\mathrm{H^+}]^2 + (k_3 K_{23}^{\mathrm{Mn}}[\mathrm{H^+}] + k_4) K_{23}^{\mathrm{T}}[\mathrm{H^+}] + (k_5 + k_6) K_{23}^{\mathrm{Mn}}[\mathrm{H^+}] + k_7 + k_8\}/AB \quad (29)$$

Integrated rate equation

The observed first-order behaviour reflected by the excellent single exponential fits to the individual stopped-flow traces is consistent with the validity of the integrated rate equation obtained from eqn. (28). Integration is carried out using the alternative form (30) of rate eqn. (28), taking into account balance condition (18) and expression (31) for the concentration of unreacted total Mn^{III}.

$$\mathrm{d[P]/d}t = k_{\mathrm{obs}}[\mathrm{Mn^{III}}]_\mathrm{T} = k[\mathrm{T}]_\mathrm{T}[\mathrm{Mn^{III}}]_\mathrm{T} \quad (30)$$

$$[\mathrm{Mn^{III}}]_\mathrm{T} = [\mathrm{Mn}]_0 - 2[\mathrm{P}]\ (\text{unreacted } \mathrm{Mn^{III}}) \quad (31)$$

where $[Mn]_0$ is the initial Mn^{III} concentration.

The integrated rate equation solved for the sum of products [P] is given by eqn. (32).

$$[\mathrm{P}] = [\mathrm{Mn}]_0\{1 - \exp(-2k_{\mathrm{obs}}{}^{\mathrm{P}}t)\} = [\mathrm{Mn}]_0\{1 - \exp(-2k[\mathrm{T}]_\mathrm{T}t)\} \quad (32)$$

The kinetic results were evaluated by fitting eqn. (29) to the experimental pH dependence of the apparent second-order rate constants k at 370 and 505 nm. eqn. (29) contains a total of nine

Table 2 Fitting results for the parameters of eqn. (29) at λ = 370 and 505 nm

Parameter	From k_{370}/M^{-1} s^{-1}	From k_{505}/M^{-1} s^{-1}	From Δk/M^{-1} s^{-1}
k_1/M^{-1} s^{-1}	$(1.01 \pm 0.11) \times 10^4$	$(1.04 \pm 0.11) \times 10^4$	0
k_2/M^{-1} s^{-1}	0	0	0
k_3/M^{-1} s^{-1}	$(9.44 \pm 0.41) \times 10^3$	$(9.60 \pm 0.38) \times 10^3$	0
k_4/M^{-1} s^{-1}	0	0	0
$k_5 + k_6$/M^{-1} s^{-1}	$(2.33 \pm 0.18) \times 10^4$	$(1.68 \pm 0.15) \times 10^4$	$(6.42 \pm 0.72) \times 10^3$ [b]
$k_7 + k_8$/M^{-1} s^{-1}	$(5.8 \pm 1.7) \times 10^2$	$(5.3 \pm 1.7) \times 10^2$	0
K_{23}^{Mn}/M^{-1} [a]	$(2.58 \pm 0.78) \times 10^3$	$(2.58 \pm 0.78) \times 10^3$	$(2.58 \pm 0.78) \times 10^3$
K_{23}^{T}/M^{-1} [a]	50.0	50.0	50.0
K_{34}^{T}/M^{-1} [a]	10.5	10.5	10.5

[a] Not varied in the fitting procedure. [b] The difference $(k_5 + k_6)_{370} - (k_5 + k_6)_{505}$ [*cf.* eqn. (33)].

parameters, *viz.* six independent rate constants (k_1 through k_4, plus $k_5 + k_6$ and $k_7 + k_8$, which cannot be separated into components) and three equilibrium constants K_{23}^{Mn}, K_{23}^{T} and K_{34}^{T}. In the fitting procedure, we used the literature values of the acid dissociation constants for the two SO_3H groups of Tiron,[16] and the value of K_{23}^{Mn} determined spectrophotometrically (Table 1). The rate constants k_2 and k_4 were neglected (set to zero) as they refer to protonated Tiron species (H_3T^- and H_4T, respectively, existing at low pH) reacting with the deprotonated Mn_1 complex formed above pH 2.5), an encounter of low probability. As a result of this approximation, the number of parameters was reduced to four, *viz.* k_1, k_3, $k_5 + k_6$ and $k_7 + k_8$. This fitting task was readily manageable using available software.

The fitting of eqn. (29) to the experimental k *vs.* pH curves obtained at λ = 370 and 505 nm (Fig. 6) afforded the rate constants listed in Table 2.

The fitting procedure has led to the remarkable result that, with the exception of $k_5 + k_6$, the individual rate constants obtained from k_{370} and k_{505}, agree within experimental error. The calculated difference curve Δk *vs.* pH (with $\Delta k = k_{370} - k_{505}$), shown in Fig. 7 can be fitted remarkably well in terms of the single variable parameter $k_5 + k_6$, keeping K_{23}^{Mn}, K_{23}^{T} and K_{34}^{T} constant. The best value for this parameter obtained from the difference curve can be approximately given by eqn. (33).

$$(k_5 + k_6)_{370} - (k_5 + k_6)_{505} = (k_5 + k_6)_{\Delta k} \qquad (33)$$

$$23300 - 16900 = 6400$$

As pictured in Scheme 1, the reaction mechanism for the catechol to *o*-quinone type oxidation of Tiron is a two-step electron transfer with a semiquinone anion radical intermediate. Owing to the lability of Mn(III), it should be of the inner-sphere type, involving prior coordination of Tiron to the Mn(III) centre. A 10-fold excess of pyrophosphate was used to stabilise $[Mn(H_2P_2O_7)_3]^{3-}$ against hydrolysis and disproportionation. In the absence of Tiron, this imparts sufficient stability to $[Mn(H_2P_2O_7)_3]^{3-}$ solutions up to pH 6. However, under reaction conditions the Tiron-catalysed disproportionation of $[Mn(H_2P_2O_7)_3]^{3-}$ takes place, which is accelerated by increasing pH. This conclusion is supported by the spectral changes accompanying the reaction. The 370 nm band characteristic of the quinone product is gradually lost from the spectra with increasing pH. Instead, a featureless spectrum is observed, which is consistent with the formation of soluble (colloidal) manganese(IV).[17]

The identical overall kinetic behaviour throughout the pH range studied points to identical kinetics of both oxidation and disproportionation, *viz.*, first-order in both Mn(III) and Tiron. Mechanistically, the difference between oxidation and disproportionation should be due to the different structures of intermediates X_1–X_5 and X_8 on the one hand, and intermediates X_6 and X_7 on the other. The two kinds of proposed structure are illustrated in Schemes 2 and 3, respectively. Oxidation occurs through a catecholato-bonded (–CO^--bonded) Tiron (Scheme 2), whereas disproportionation takes place *via* –SO_2O^--bonded Tiron (Scheme 3). The catalytic effect of Tiron on the disproportionation of $[Mn(H_2P_2O_7)_3]^{3-}$ is due to the good leaving-group character of its SO_2O^--bonded isomer, facilitating the conversion of intermediates X_6 and X_7 to a hydroxo derivative (Scheme 3). The observed pattern is supported by the lack of $[Mn(H_2P_2O_7)_3]^{3-}$ hydrolysis/disproportionation in the absence of Tiron at identical pHs.

The complete displacement of the pyrophosphato ligand does not take place, unidentate species only being formed. This is in line with the lack of retardation of the reaction upon increasing the excess of pyrophosphate over manganese(III).

Acknowledgements

This work was supported by the Hungarian Research Fund (OTKA grant no. T 023219).

References

1 L. Que, Jr., in *Bioinorganic Catalysis*, ed. J. Reedijk and E. Bouwman, Marcel Dekker, New York, Basel, 2nd edn., 1999, ch. 10, pp. 269–321.
2 (*a*) T. Funabiki, in *Oxygenases and Model Systems*, ed. T. Funabiki, Kluwer, Dordrecht, Boston, London, 1997, ch. 2, pp. 19–104; (*b*) T. Funabiki, in *Oxygenases and Model Systems*, ed. T. Funabiki, Kluwer, Dordrecht, Boston, London, 1997, ch. 3, pp. 105–155.
3 (*a*) L. I. Simándi and T. L. Simándi, *J. Chem. Soc., Dalton Trans.*, 1998, 3275; (*b*) T. L. Simándi and L. I. Simándi, *J. Chem. Soc., Dalton Trans.*, 1999, 4529.
4 L. Que, Jr. and M. F. Reynolds, in *Metal Ions in Biological Systems*, ed. A. Sigel and H. Sigel, Marcel Dekker, New York, Basel, 2000, vol. 37, ch. 15, pp. 505–525.
5 V. Kahn and R. W. Miller, *Phytochemistry*, 1987, **26**, 2459.
6 G. Davies, *Coord. Chem. Rev.*, 1969, **4**, 199.
7 H. Diebler and N. Sutin, *J. Phys. Chem.*, 1964, **68**, 174.
8 J. I. Watters and I. M. Kolthoff, *J. Am. Chem. Soc.*, 1948, **70**, 2455.
9 (*a*) R. E. Hamm and M. A. Suvyn, *Inorg. Chem.*, 1967, **6**, 139; (*b*) Y. Yoshino, A. Ouchi, Y. Tsunoda and M. Kojima, *Can. J. Chem.*, 1962, **40**, 775.
10 W. A. Waters and J. S. Littler, in *Oxidation in Organic Chemistry*, ed. K. B. Wiberg, Academic Press, New York, 1965, pp. 185–241.
11 (*a*) E. Mentasti, E. Pelizetti, E. Pramauro and G. Giraudi, *Inorg. Chim. Acta*, 1975, **12**, 61; (*b*) E. Pelizetti, E. Mentasti and G. Giraudi, *Inorg. Chim. Acta*, 1975, **15**, L1; (*c*) G. Davies, *Inorg. Chim. Acta*, 1975, **14**, L13; (*d*) E. Pelizetti, E. Mentasti and E. Pramauro, *J. Chem. Soc., Dalton Trans.*, 1978, 61.
12 (*a*) G. Giraudi and E. Mentasti, *Transition Met. Chem.*, 1981, **6**, 230; (*b*) P. Arselli and E. Mentasti, *J. Chem. Soc., Dalton Trans.*, 1983, 689.
13 (*a*) M. Jáky and L. I. Simándi, *J. Chem. Soc., Perkin Trans. 2*, 1972, 1481; M. Jáky and L. I. Simándi, *J. Chem. Soc., Perkin Trans. 2*, 1976, 939; (*b*) L. I. Simándi and M. Jáky, *J. Chem. Soc., Perkin Trans. 2*, 1972, 2326; L. I. Simándi and M. Jáky, *J. Chem. Soc., Perkin Trans. 2*, 1973, 1856; L. I. Simándi and M. Jáky, *J. Chem. Soc., Perkin Trans. 2*, 1973, 1861; (*c*) M. Jáky, L. I. Simándi, L. Maros and I. Molnár-Perl, *J. Chem. Soc., Perkin Trans. 2*, 1973, 1565; (*d*) L. I. Simándi and M. Jáky, *J. Am. Chem. Soc.*, 1976, **98**, 1995; (*e*) Z. Szeverényi, L. I. Simándi and M. Jáky, *Inorg. Chim. Acta*, 1977, **23**, L31; (*f*) L. I. Simándi, M. Jáky, N. T. Son and

J. Hegedüs-Vajda, *J. Chem. Soc., Perkin Trans. 2*, 1977, 1794; (*g*) M. Jáky, Z. Szeverényi and L. I. Simándi, *Inorg. Chim. Acta*, 1991, **186**, 33.
14 (*a*) I. K. Bhat, B. S. Sherigara and I. Pinto, *Transition Met. Chem.*, 1993, **18**, 163; (*b*) S. Chandraju, B. S. Sherigara and N. M. Made Gowda, *Int. J. Chem. Kinet.*, 1994, **26**, 1105; (*c*) B. S. Sherigara, K. I. Bhat, I. Pinto and N. M. Made Gowda, *Int. J. Chem. Kinet.*, 1995, **27**, 675.
15 (*a*) I. M. Kolthoff and J. I. Watters, *Ind. Eng. Chem. Anal. Ed.*, 1943, **15**, 8; I. M. Kolthoff and J. I. Watters, *Ind. Eng. Chem. Anal. Ed.*, 1944, **16**, 187; (*b*) V. I. Gordienko, V. I. Sidorenko and I. I. Mikhalyuk, *Zh. Neorg. Khim.*, 1970, **15**, 2397; (*c*) I. K. Bhat, B. S. Sherigara and I. Pinto, *Transition Met. Chem.*, 1993, **18**, 163.
16 A. F. Dzhelassi and A. M. Egorov, *Zh. Fiz. Khim.*, 1969, **43**, 240.
17 L. I. Simándi, M. Jáky, C. R. Savage and Z. A. Schelly, *J. Am. Chem. Soc.*, 1985, **107**, 4220.